Sequestration of toxic Pb(II) ions by chemically treated rubber (*Hevea brasiliensis*) leaf powder

Megat Hanafiah Megat Ahmad Kamal[1,*], Wan Mat Khalir Wan Khaima Azira[2], Mohamed Kasmawati[2], Zakaria Haslizaidi[1], Wan Ngah Wan Saime[3]

1. Faculty of Applied Sciences, Universiti Teknologi MARA Pahang, 26400 Jengka, Pahang, Malaysia. E-mail: makmh73@yahoo.com.my
2. Faculty of Applied Sciences, Universiti Teknologi MARA, 40450 Shah Alam, Selangor, Malaysia
3. School of Chemical Sciences, Universiti Sains Malaysia, 11800 Minden, Penang, Malaysia

Abstract

Rubber leaf powder (an agricultural waste) was treated with potassium permanganate followed by sodium carbonate and its performance in the removal of Pb(II) ions from aqueous solution was evaluated. The interactions between Pb(II) ions and functional groups on the adsorbent surface were confirmed by Fourier transform infrared (FT-IR) spectroscopy, scanning electron microscopy (SEM) coupled with X-ray energy dispersive spectroscopy (EDX). The effects of several important parameters which can affect adsorption capacity such as pH, adsorbent dosage, initial lead concentration and contact time were studied. The optimum pH range for lead adsorption was 4–5. Even at very low adsorbent dosage of 0.02 g, almost 100% of Pb(II) ions (23 mg/L) could be removed. The adsorption capacity was also dependent on lead concentration and contact time, and relatively a short period of time (60–90 min) was required to reach equilibrium. The equilibrium data were analyzed with Langmuir, Freundlich and Dubinin-Radushkevich isotherms. Based on Langmuir model, the maximum adsorption capacity of lead was 95.3 mg/g. Three kinetic models including pseudo first-order, pseudo second-order and Boyd were used to analyze the lead adsorption process, and the results showed that the pseudo second-order fitted well with correlation coefficients greater than 0.99.

Key words: adsorption; isotherm; kinetics; lead; rubber leaf powder

DOI: 10.1016/S1001-0742(09)60101-7

Introduction

Lead in the environment commonly originated from various kinds of industrial activities such as mining, smelting and metal plating, battery manufacturing, ammunition production, paint production and paper and pulp processing. Lead has been identified as one of the most toxic heavy metals due to its detrimental effects on human nervous system, blood circulation system, kidneys and reproductive system (Tunali et al., 2006; Li et al., 2009). Therefore, lead in industrial wastewaters must be properly treated to prevent it from reaching water bodies. Adsorption is a well known and preferable technique commonly applied in the removal of heavy metal ions compared to conventional methods such as chemical precipitation, electroflotation, flocculation, ion-exchange and reverse osmosis. Different types of adsorbents derived from agricultural wastes have been used to adsorb Pb(II) ions (Bailey et al., 1999; Gupta and Bhattacharyya, 2008; Li et al., 2009; Lee et al., 1999; Bulut and Tez, 2007). Not only that agricultural wastes are cheap and abundant; they are also rich in cellulose, lignin, pectin and tannin which can serve as the adsorption sites

for heavy metal ions.

In recent years, for the purpose of enhancing the adsorption capacities of heavy metal ions and improving the recyclability of adsorbents, chemical modifications of adsorbents have attracted the attention of many researchers. The summary of applications of various types of chemically modified plant wastes in removing heavy metal ions have been reported by Wan Ngah and Hanafiah (2008a), O'Connell et al. (2008), Lesmana et al. (2008) and Arief et al. (2008). In this work, rubber (*Hevea brasiliensis*) leaf powder was selected as an adsorbent for lead adsorption. Rubber trees are widely planted in tropical countries mainly Brazil, Malaysia, Indonesia, Thailand and India for latex, a raw material for producing rubber gloves, tyres, shoes, etc. In Malaysia, more than 1.2×10^6 ha of lands are planted with rubber trees, making rubber one of the most important commodities. However, large quantities of solid wastes are also generated from rubber plantations. Therefore, this work focused on the application of a solid waste (rubber leaves) in the treatment of liquid waste containing Pb(II) ions. A previous work indicated that 46 mg/g of lead could be adsorbed by untreated rubber leaf powder (Hanafiah et al., 2006). The main objective of this work

---

* Corresponding author. E-mail: makmh73@yahoo.com.my

was to improve the adsorption capacity by oxidizing the primary alcohol groups in rubber leaf powder to carboxylic groups using potassium permanganate ($KMnO_4$) solution. This type of chemical treatment has been conducted by Luo et al. (2006), Basha et al. (2008), Basha and Murthy (2007) and Liu et al. (2009) to improve adsorption capacity of heavy metal ions by various types of biomass. Then, a further treatment with a strong alkaline solution (Na_2CO_3) was carried out to introduce more Lewis base (–$RCOO^-$ and –RO^-) groups on the adsorbent surface.

1 Materials and methods

1.1 Chemical treatment of rubber (*Hevea brasiliensis*) leaf powder

Fresh mature rubber leaves (light brown in color) were collected from Universiti Teknologi MARA Pahang rubber plantation, Malaysia. The leaves were washed with tap water to remove dust and soluble impurities, dried overnight in an oven at 105°C, ground and sieved to obtain particle size of 355–500 μm. Preparation of the chemically treated rubber leaf powder was carried out using potassium permanganate ($KMnO_4$) and sodium carbonate (Na_2CO_3) solutions as follows: 10 g of dried rubber leaf powder and 200 mL (0.10 mol/L) $KMnO_4$ solution were mixed in a 250-mL conical flask. This type of treatment will oxidize the primary alcohol groups on rubber leaf surface to carboxylic groups. The mixture was shaken at 250 r/min for 2 hr at room temperature (24.0 ± 0.5)°C. The mixture was filtered with a vacuum pump and the treated leaf powder was washed extensively with deionized water, and then dried in an oven at 80°C overnight. The dried leaf powder was further treated with 200 mL (0.10 mol/L) Na_2CO_3 solution in a 250-mL conical flask, shaken at 250 r/min for 2 hr at room temperature (24.0 ± 0.5)°C. This type of treatment will cause the conversion of carboxylic acid (–RCOOH), ester (–RCOOR') and unreacted hydroxyl (-ROH) groups to –COO^-Na^+ and –RO^-Na^+. The mixture was filtered by using a vacuum pump and the leaf powder was washed extensively with deionized water to remove excess base. The sodium carbonate treated rubber leaf powder was again dried in an oven at 80°C overnight, stored in a glass bottle for further experiments and was designated as chemically treated rubber leaf powder (CTRL).

1.2 Characterization of CTRL

Characterization of CTRL was carried out to understand the mechanisms of lead adsorption. Identification of the functional groups in CTRL was performed by using Fourier transform infrared spectrophotometer (FT-IR, System 1600, PerkinElmer, USA). The pH of aqueous slurry was carried out according to the previous method described by Wan Ngah and Hanafiah (2008b). Determination of pH_{ZPC} of CTRL was done according to the method reported by Balistrieri and Murray (1981). The surface morphology of CTRL was observed by scanning electron microscope (SEM; LeoSupra VP50, Carl-Zeiss SMT, Germany) coupled with X-ray energy dispersive spectrometer (EDX).

The adsorbent was coated with gold and bombarded with electrons accelerated by 15 keV power supply. Determination of ash content was carried out by combusting 1.0 g CTRL at 600°C in a furnace for 2 hr.

1.3 Lead adsorption experiments

All batch adsorption experiments were carried out in duplicates and the results were reported as average. All chemicals used were of analytical reagent grade. The standard solution of lead (1000 mg/L) was obtained from Merck (Germany). Experimental solutions of the desired lead concentration were obtained by successive dilutions. For adsorption experiments, a known weight of CTRL was mixed with 50 mL lead solutions in stoppered conical flasks at room temperature (24.0 ± 0.5)°C, shaken at 250 r/min for a certain period of time. The initial pH of lead solution was fixed at 4 by adding 1 mol/L HCl or NaOH solutions. The effect of pH was carried out over a pH range 2–5 to avoid the precipitation of Pb(OH)$_2$ which starts to occur at pH 5.8 (Tiwari et al., 2007). To study the effect of dosage, the weight of adsorbent was varied from 0.01 to 0.10 g. The effects of lead concentration and contact time were conducted by shaking CTRL with lead solutions (23, 33 and 43 mg/L) at various time intervals (0–120 min). The isotherm study was conducted by equilibrating lead solutions (13–60 mg/L) with 0.02 g CTRL. After adsorption, the mixtures were vacuum-filtered and the filtrates were analyzed for Pb content using an inductively coupled plasma-optical emission spectrometer (ICP-OES; Optima 5300 DV, Perkin Elmer, USA). The amount of lead adsorbed, q_e, (mg/g) and percentage of removal were calculated by using the following Eqs. (1) and (2):

$$q_e = \frac{C_0 - C_e}{m} \times V \tag{1}$$

$$R = \frac{C_0 - C_e}{C_o} \times 100\% \tag{2}$$

where, C_o (mg/L) and C_e (mg/L) are lead concentrations before and after adsorption, respectively; V (L) is the volume of lead solution, and m (g) is the weight of CTRL.

2 Results and discussion

2.1 Adsorbent characterization

CTRL is slightly basic as the pH value of aqueous slurry was 8.11. The high ash content of 20.4% could indicate the presence of high amount of metallic elements in CTRL, which would form metal oxides upon combustion. The pH_{ZPC} is a characteristic that determines the pH at which the adsorbent surface has net electrical neutrality and it can give important information on electrostatic interactions between adsorbent and adsorbate. The pH_{ZPC} plot is shown in Fig. 1 and was determined as 8.45. At this value, the acidic or basic functional groups no longer contribute to the pH of the solution. If the solution pH is higher than pH_{ZPC}, the adsorbent surface will carry negative charge and vice versa. Therefore, cations adsorption will be more favourable at pH value higher than pH_{ZPC}.
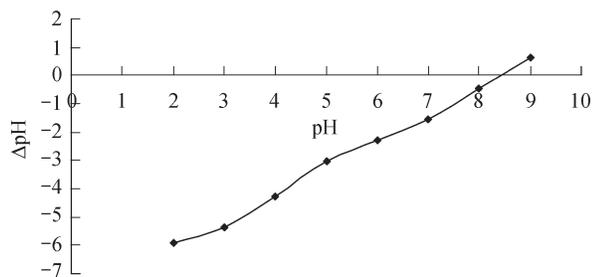
Fig. 1 pH$_{ZPC}$ plot of chemically treated rubber leaf powder (CTRL).

The FT-IR analysis was carried out to identify the functional groups in CTRL that might be involved in the adsorption process. A comparison of FT-IR spectra of unloaded and lead loaded CTRL is shown in Fig. 2. The spectrum of CTRL (Fig. 2a) displays a number of absorption peaks, which indicates the complex nature of the adsorbent. The broad and strong band ranging from 3000 to 3600 cm^{-1} indicates the overlapping of Si–OH (silanol), R–OH (hydroxyl) and –NH$_2$ (amine) stretching vibrations. The peaks observed at 2922 and 2851 cm^{-1} can be assigned to asymmetric and symmetric –CH$_2$ groups. The peaks located at 1735 and 1719 cm^{-1} are characteristic of carbonyl group stretching from carboxylic acid or ester group. The peak at 1636 cm^{-1} corresponds to the carboxylate (–COO$^-$) and C=C stretching that can be attributed to the aromatic bond (Farinella et al., 2006). The small peak observed at 1517 cm^{-1} is due to –NH$_2$ group (Ncibi et al., 2006) and C=C stretching of aromatic rings of lignin. The wavenumbers from 1400 to 1600 cm^{-1} are assigned to aromatic skeletal vibration. The peaks at 1054 and 1162 cm^{-1} are assigned to alcoholic C–O and C–N stretching vibrations, respectively; while peaks around 1109–1264 cm^{-1} correspond to phenolic hydroxyl groups in lignin. The small peak at 1384 cm^{-1} indicates the presence of carboxylate group. The strong peak observed at 1054 cm^{-1}

could also represent C–O–C of ether group. The region below 1000 cm^{-1} is called "fingerprint region" and the adsorption cannot be clearly assigned to any particular vibration because they correspond to complex interacting vibration systems. The FT-IR spectrum of lead-loaded CTRL (Fig. 2b) shows some shift in wavenumbers. For instance, the wavenumber at 3355 cm^{-1} shifted to 3397 cm^{-1} after lead adsorption, suggesting the participation of –OH and –NH$_2$ in forming complexes with Pb(II) ions. The intensity of the peaks at 1735 and 1719 cm^{-1} were reduced while the peak at 1636 cm^{-1} shifted to 1629 cm^{-1}. The sharp peak at 1384 cm^{-1} further confirmed the participation of carboxylate group in binding Pb(II) ions. Based on the shift in the wavenumbers as indicated by the FT-IR spectra, functional groups of –OH, –NH$_2$, –COOH, C=C and –COO$^-$ could act as important adsorption sites for lead ions.

SEM and EDX are useful tools for evaluating the elemental characteristics of the adsorbents and these two techniques have been widely used in heavy metals adsorption studies especially in determining the adsorption mechanism (Akar and Tunali, 2005; Tunali et al., 2006; Panda et al., 2007; Pino et al., 2006). The SEM images and EDX spectra for CTRL before and after lead adsorption are shown in Fig. 3. The SEM images (at 500× magnification) show the rough surface and porosity of CTRL, conditions which might favour the adsorption of Pb(II) ions. The EDX spectrum for CTRL before adsorption (Fig. 3a) showed some peaks for inorganic (Na, K, Ca, Mg and Mn) species. The presence of K and Mn on CTRL surface could originate from KMnO$_4$ solution used during treatment. Although the surface of the CTRL before and after lead adsorption looks very similar, the EDX analysis gave different results and this analysis could be used to confirm the attachment of Pb(II) ions onto CTRL. The presence of lead on CTRL surface is represented by the peak at
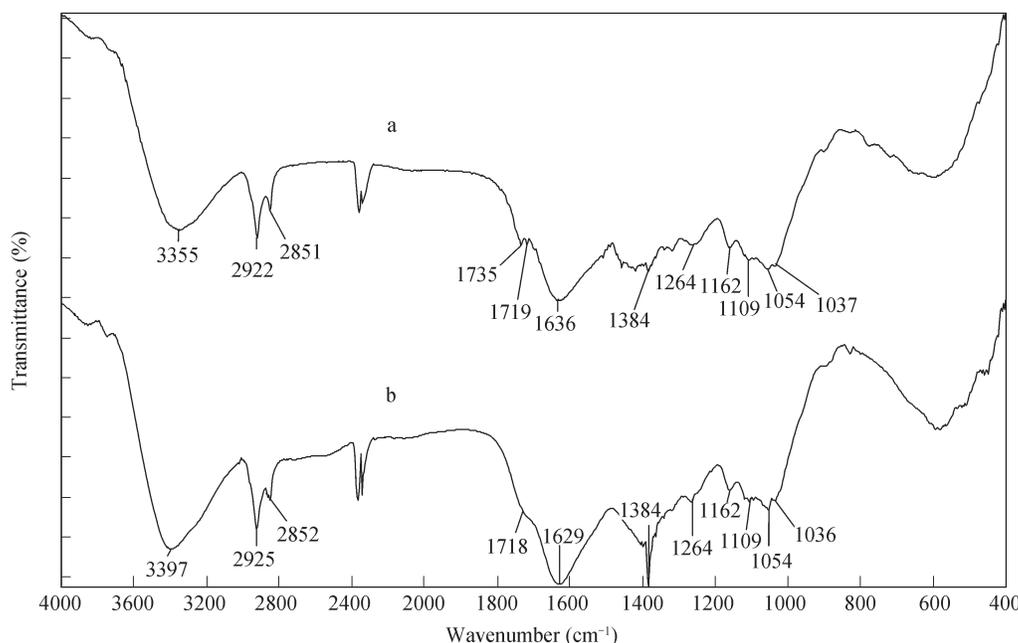

Fig. 2 FT-IR spectra of CTRL before (a) and after (b) lead adsorption.
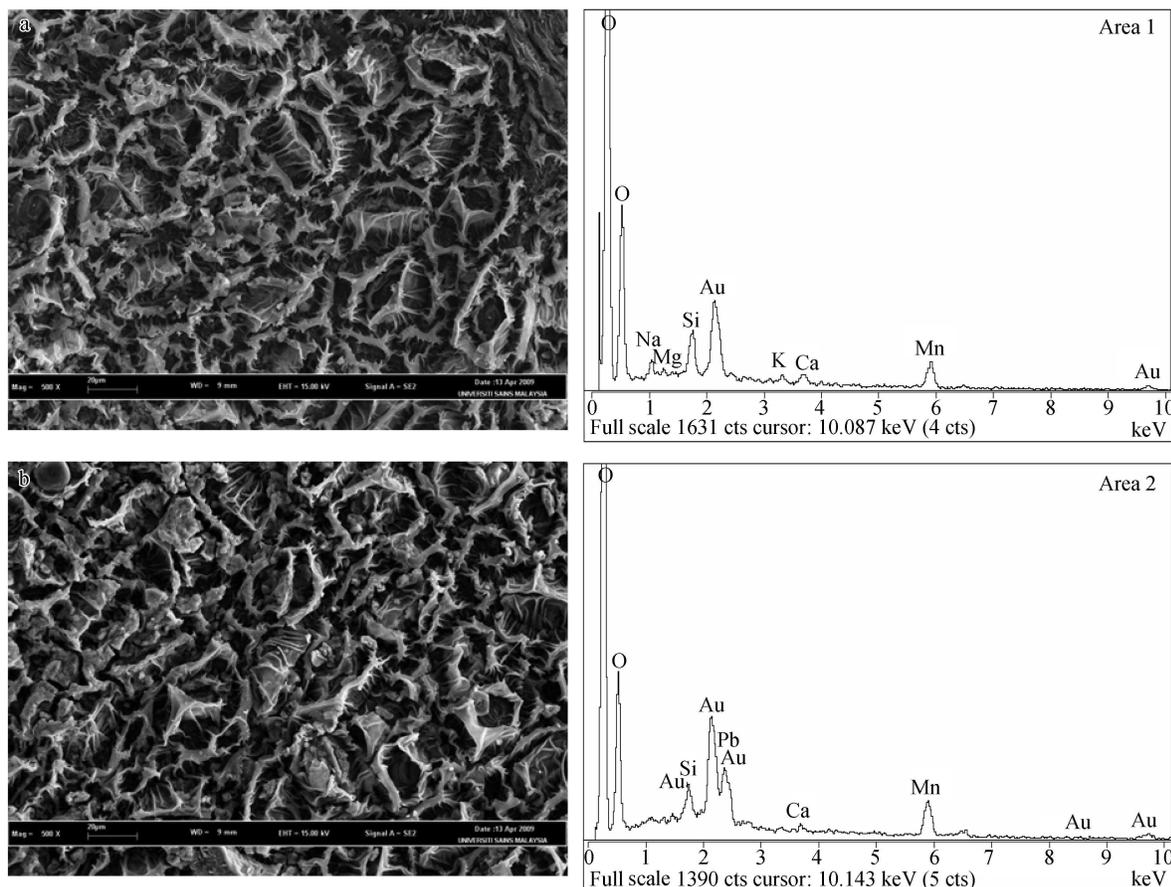
Fig. 3   SEM images at 500× magnification and EDX spectra of CTRL before (a) and after (b) lead adsorption.

2.3 keV (Fig. 3b). The peaks at about 1.1, 1.3 and 3.3 keV corresponding to Na^+, Mg^{2+} and K^+ ions, respectively, disappeared after Pb adsorption while the intensity of Ca peak at 3.7 keV decreased. The disappearance of light metal peaks and the appearance of Pb peak as revealed by EDX spectra indicated that ion-exchange could also be involved during adsorption process. This kind of observation has also been reported in our previous studies (Wan Ngah and Hanafiah, 2009, 2008b, 2008c; Hanafiah et al., 2009) and by other researchers (Akar and Tunali, 2005; Panda et al., 2007). The presence of Au peaks in both spectra is due to the gold purposely settled to increase electric conduction and to improve the quality of the images.

2.2 Effect of pH

The pH of lead solution is one of the most important variables in adsorption process since pH can affect both the chemical speciation of lead ions and the ionization state of functional groups (carboxyl, amino, hydroxyl, etc.) on the adsorbent surface. Adsorption experiments were not conducted at pH beyond 5 due to the possible precipitation of $Pb(OH)_2$ and to ensure that only Pb^{2+} species involved in adsorption (Lee et al., 1999). The result for the effect of pH on lead adsorption is shown in Fig. 4 and in general, the adsorption capacities increased with increasing pH values. The lowest amount of lead adsorbed occurred at pH 2 (8.4 mg/g) and the highest at pH 5 (58.6 mg/g). At pH 2, Pb(II) ions had to compete with a large number of H_3O^+
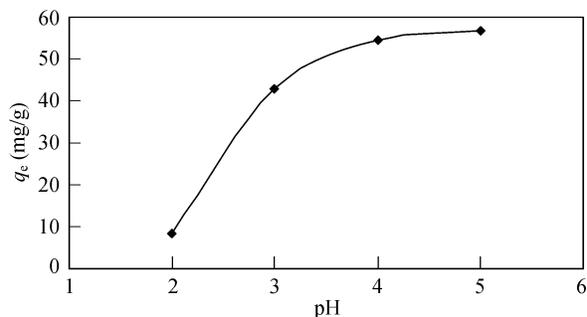

Fig. 4   Effect of pH on lead adsorption by CTRL (adsorbent weight: 0.02 g, volume: 50 mL, shaking speed: 250 r/min, equilibrium time: 90 min, Pb concentration: 23 mg/L).

ions for adsorption sites; therefore, the adsorption capacity of lead was low. As pH increased, the competing effect of H_3O^+ ions decreases due to the lower concentration of H_3O^+ ions and the positively Pb(II) ions could easily adsorb on the available adsorption sites of the adsorbents. The region where there is a sharp increase in adsorption capacity from low to high pH can be called pH adsorption edge (Upendra and Bandyopadhyay, 2006). In this study, the pH adsorption edge was 2–4.

2.3 Effect of adsorbent dosage

The effect of adsorbent dosage on percentage of lead removal is shown in Fig. 5. It is apparent that by increasing
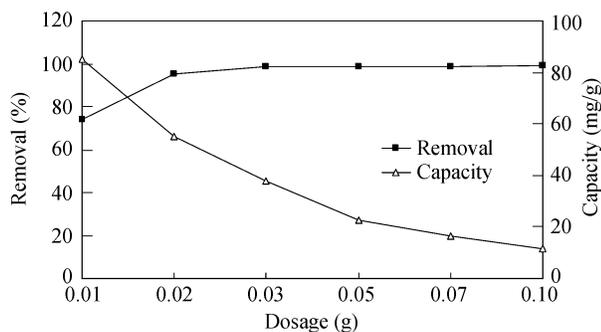
Fig. 5 Effect of adsorbent dosage on lead adsorption by CTRL (volume: 50 mL; pH: 4; shaking speed: 250 r/min; equilibrium time: 90 min; Pb concentration: 23 mg/L).

Fig. 6 Effect of initial lead concentration and contact time on lead adsorption by CTRL (adsorbent weight: 0.02 g; pH: 4; volume: 50 mL; shaking speed: 250 r/min).

the dosage, the percentage of removal increased but remained constant beyond dosage of 0.02 g. The lowest removal was 74.2% and reached maximum at dosage of 0.1 g (99%). The increase in percentage of removal as dosage was increased was due to the increase in the surface area of CTRL. A higher adsorbent dosage also reflects a greater number of available adsorption sites (Vijayaraghavan et al., 2006), therefore, more lead ions were able to be adsorbed. On the other hand, the adsorption capacity decreased with the increase in adsorbent dosage. It is important to note that the concentration of lead was fixed while the adsorbent dosage was increased. Therefore, as the dosage increased, the ratio of number of adsorption sites to the number of heavy metal ions would increase and there would be plenty of unadsorbed adsorption sites. Another possible reason could be due to the particle aggregation, which would lead to a decrease in total surface area of the adsorbent (Shukla et al., 2002). According to Balasubramaniam et al. (2009), the adsorption capacity and percentage of removal are equally important in adsorption experiments because both factors usually take part in deciding the adsorption performance of a given adsorbent. The adsorbent dosage of 0.02 g was selected for further adsorption studies because it showed both relatively high percentage of removal and high adsorption capacity.

2.4 Effect of lead concentration and contact time

The lead concentration and contact time are important factors in adsorption kinetic because they determine the time required to transport adsorbates to the adsorption sites. It can be clearly seen in Fig. 6 that the adsorption capacity and equilibrium time are dependent on lead concentration. In general, all the plots showed that the rate of adsorption of Pb(II) ions consisted of two phases; an initial rapid phase where adsorption was fast and a second slower phase where equilibrium uptake was achieved. The first phase was related to external surface adsorption, which occurred instantaneously and the second phase was the gradual adsorption stage before the uptake of lead reached equilibrium. The high adsorption rate represented by the steep slopes of the curves at the initial period of 5 min was due to the availability of uncovered adsorption sites. As these sites were progressively covered by lead ions, the adsorption rate became slower until the equilibrium uptake was achieved.
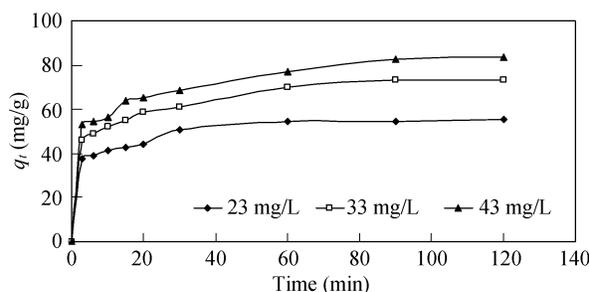
The adsorption capacities increased as the concentrations and contact time increased. According to Malkoc and Nuhoglu (2005), the initial concentration provided an important driving force to overcome the mass transfer resistance between the aqueous and solid phases. As the concentration increased, a better driving force was achieved and a higher probability of collision between adsorbate and adsorbent surface occurred (Ozsoy and Kumbur, 2006). It took only 30 min to reach equilibrium for the lowest concentration (23 mg/L) of lead ions. At low concentration, the ratio of lead ions to the number of available adsorption sites is low; hence the adsorption sites seemed to take up available lead ions much quickly due to less competition among lead ions (Gupta and Bhattacharyya, 2008). The maximum adsorption capacities recorded at 23, 33 and 43 mg/L were 55.6, 73.3 and 83.4 mg/g, respectively. Overall, CTRL showed that equilibrium was achieved at relatively short period of time (< 90 min), which is a very important criterion for economical wastewater treatment plant application (Kadirvelu and Namasivayam, 2003).

2.5 Adsorption kinetic models

Adsorption kinetic describes the rate of heavy metal ions uptake on an adsorbent and is useful in providing information on the rate determining steps (film diffusion, chemical reactions or intraparticle diffusion). The three most common kinetic models applied in adsorption studies are pseudo first-order (Ho and McKay, 1998), pseudo second-order (Ho and McKay, 2000), and Boyd (Boyd et al., 1947); given by Eqs. (3), (4), and (5)–(8), respectively:

$$\log(q_e - q_t) = \log q_e - \frac{k_1}{2.303}t \qquad (3)$$

$$\frac{t}{q_t} = \frac{1}{h} + \frac{1}{q_e}t \qquad (4)$$

$$F = 1 - \frac{6}{\pi^2} \sum_{n=1}^{\infty} \frac{1}{n^2}(\exp) - n^2 B_t \qquad (5)$$

$$F = \frac{q_t}{q_\infty} \qquad (6)$$

$$B = \frac{\pi^2 D_i}{r^2} \qquad (7)$$

$$B_t = -0.4977 - \ln(1 - \frac{q_t}{q_\infty}) \qquad (8)$$

where, q_t (mg/g) and q_e (mg/g) are the amount of lead adsorbed at time t (min) and at equilibrium, respectively; k_1 (min^{-1}) is the rate constant of the pseudo first-order adsorption process, $h = k_2q_e^2$ can be regarded as the initial adsorption rate as $t \longrightarrow 0$, k_2 (g/(mg·min)) is the rate constant of pseudo second-order adsorption, F represents the fraction of lead adsorbed at any time t (min), q_∞ (mg/g) is the amount of lead adsorbed at infinite time, n is an integer, B_t is a mathematical function of F, and r (cm) represents the radius of adsorbent by assuming spherical particles. The B value can be obtained from the slope of the plot B_t versus t, and D_i (cm^2/s) is the effective diffusion coefficient.

The pseudo first-order, pseudo second-order and Boyd plots are shown in Figs. 7 and 8, respectively; while the rate constants and correlation coefficients are shown in Table 1. The pseudo first-order plots are linear with R^2 close to unity, however, the calculated values of adsorption capacities ($q_{e,cal}$) are lower than the experimental values ($q_{e,exp}$). The pseudo second-order plots are also linear with

$q_{e,cal}$ and $q_{e,exp}$ values close to each other. This suggests that pseudo second-order model was better fitted than pseudo first-order and chemical reactions (chemisorption or ion-exchange) could be the rate determining steps. The Boyd plots are found to be nonlinear and they do not pass the origin, an indication that film diffusion is another rate determining step. This is further confirmed by the D_i values (2.7×10^{-6}–3.0×10^{-6} cm^2/s) in Table 1, which are much higher than the intraparticle diffusion range (10^{-11}–10^{-13} cm^2/s).

2.6 Adsorption isotherms

Adsorption isotherm is an expression that shows the relationship between amount of adsorbate adsorbed per unit weight of adsorbent (q_e, mg/g) and the concentration of adsorbate in bulk solution (C_e, mg/L) at a given temperature under equilibrium conditions. Adsorption equilibrium is established when the amount of adsorbate being adsorbed is equal to the amount being desorbed from the adsorbent. At this stage, the equilibrium concentrations in both phases are constant. Adsorption isotherm is very useful in giving information on adsorption mechanisms, surface properties and affinity of an adsorbent towards heavy metal ions (Ho et al., 2002). The experimental adsorption isotherm data of lead ions on CTRL is shown in Fig. 8. In general, the plots clearly indicate that with an increase in initial lead concentrations, the adsorption capacities also increased. A steeper slope of the curve can be observed at lower initial lead concentrations (< 30 mg/L) before reaching a plateau at higher concentrations (> 40 mg/L). This means that at lower concentrations, CTRL had sufficient number of adsorption sites to adsorb lead ions. At higher concentrations, however, the ratio of the number of lead ions to the number of adsorption sites increased, thus adsorption sites would be saturated. It is also important to note the shape of the isotherm which can provide some information
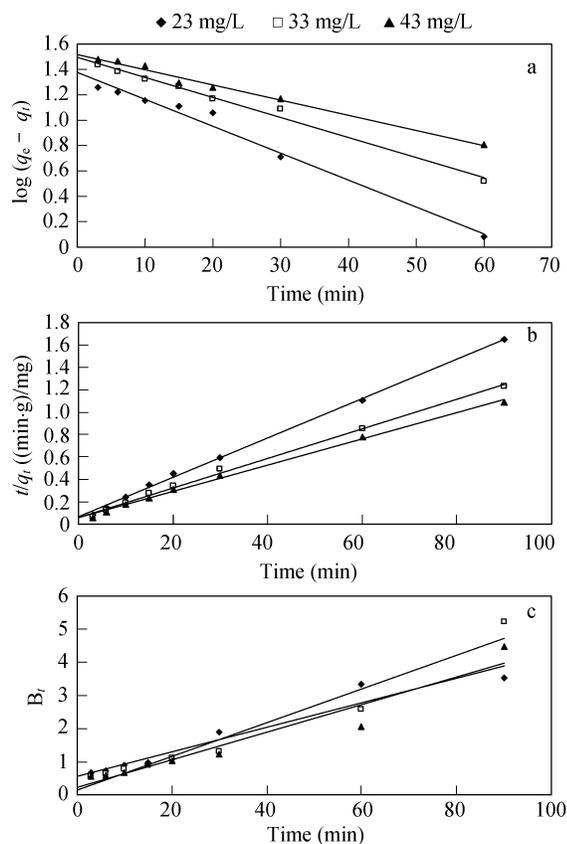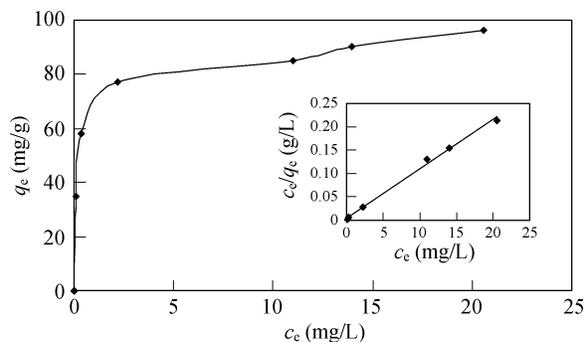

Fig. 7 Pseudo first-order (a), second-order (b), Boyd (c) kinetic plots of lead adsorption by CTRL (adsorbent weight: 0.02 g; pH: 4; volume: 50 mL; shaking speed: 250 r/min).

Fig. 8 Adsorption isotherm plot. Inset: linearized Langmuir plot (adsorbent weight: 0.02 g, pH: 4, volume: 50 mL, shaking speed: 250 r/min, Pb concentration: 13–60 mg/L, equilibrium time: 90 min).

Table 1   Pseudo first-order, pseudo second-order and Boyd constants at different concentrations of Pb(II)

Pb conc. (mg/L)	$q_{e,exp}$ (mg/g)	Pseudo first-order			Pseudo second-order				Boyd	
		$q_{e,cal}$ (mg/g)	k_1 (min^{-1})	R^2	h (mg/(g·min))	k_2 (mg/(min·g))	$q_{e,cal}$ (mg/g)	R^2	D_i (cm^2/s)	R^2
23	55.6	23.9	4.9×10^{-2}	0.988	15.9	4.9×10^{-3}	56.8	0.998	2.7×10^{-6}	0.943
33	73.3	31.2	3.6×10^{-2}	0.991	16.6	2.9×10^{-3}	75.8	0.997	3.7×10^{-6}	0.951
43	83.4	32.9	2.7×10^{-2}	0.982	18.2	2.5×10^{-3}	84.8	0.996	3.0×10^{-6}	0.933

Table 2   Langmuir, Freundlich and Dubinin-Radushkevich isotherm constants and correlation coefficients

Langmuir			Freundlich			Dubinin-Radushkevich		
q_{max} (mg/g)	b (L/mg)	R^2	K_F (mg/g)	n	R^2	q_m (mg/g)	E (kJ/mol)	R^2
95.3	2.2	0.996	60.2	6.1	0.917	177.7	20.4	0.942

on adsorbate-adsorbent interaction. The plot obtained is "H" type isotherm in Giles classification system (Giles et al., 1974). The H-type isotherm usually indicates chemical adsorption (chemisorption) and reflects a relatively high affinity or strong interaction between adsorbate and the adsorbent.

The isotherm data were further analyzed with three most common isotherm models: Langmuir, Freundlich and Dubinin-Radushkevich. Langmuir isotherm is probably the most widely applied isotherm model in many adsorption studies. The model was developed based on assumptions that adsorption occurs at specific homogeneous sites on the adsorbent (Langmuir, 1916) and was used successfully in many monolayer adsorption processes. It also assumes no transmigration of adsorbate in the plane of adsorbent surface. The Langmuir equation can be written as Eqs. (9) and (10):

$$q_e = \frac{q_{max}bC_e}{(1 + bC_e)} \quad \text{(non-linear form)} \tag{9}$$

$$\frac{C_e}{q_e} = \frac{1}{q_{max}b} + \frac{C_e}{q_{max}} \quad \text{(linear form)} \tag{10}$$

where, q_{max} (mg/g) is the maximum adsorption capacity and b (L/mg) is a constant related to energy of adsorption which quantitatively reflects the affinity between the adsorbent and adsorbate. Therefore, a plot of C_e/q_e versus C_e gives a straight line of slope $1/q_{max}$ and intercept $1/(q_{max}b)$. The Langmuir plot of lead ions is shown in Fig. 8 and the summary of the Langmuir constants (b), maximum adsorption capacity and correlation coefficient is shown in Table 2. The maximum adsorption capacity is 95.3 mg/g, which is almost similar to the experimental value (96.1 mg/g). The R^2 value was close to unity, indicating isotherm data fitted well to the Langmuir plot.

Freundlich isotherm gives the relationship between equilibrium liquid and solid phase capacity based on the multilayer adsorption (heterogeneous surface). This isotherm is derived from the assumption that the adsorption sites are distributed exponentially with respect to the heat of adsorption. It also assumes that the stronger adsorption sites are occupied first and the binding strength decreases with the increasing degree of site occupation. The Freundlich model is given by (Freundlich, 1906):

$$q_e = K_F C_e^{1/n} \quad \text{(non-linear form)} \tag{11}$$

$$\log q_e = \log K_F + \frac{1}{n}\log C_e \quad \text{(linear form)} \tag{12}$$

where, K_F (mg/g) represents adsorption capacity and n is related to adsorption intensity (unitless). If the value of n is greater than unity, this is an indication of a favourable adsorption. A plot of $\log q_e$ versus $\log C_e$ will give a straight line of slope $1/n$ and intercept K_F (plot not shown). The maximum adsorption capacities (K_F) of lead ions based on

Freundlich model, the adsorption intensity value (n) and correlation coefficient are given in Table 2. Although the value of n is greater than 1, the K_F value (60.2 mg/g) is far much lower than the experimental adsorption capacity while the R^2 value of 0.917 indicates that adsorption of lead ions did not fit well Freundlich model.

Dubinin-Radushkecivh (D-R) isotherm was applied to distinguish between physical and chemical adsorption. The linear form of D-R isotherm equation is given by (Dubinin et al., 1947):

$$\ln q_e = \ln q_m - K\varepsilon^2 \tag{13}$$

where, ε (Polanyi potential) is equal to $RT\ln(1+1/C_e)$, R is the gas constant (8.314 J/(mol·K)), and T (K) is the temperature, q_m (mg/g) is the maximum adsorption capacity based on D-R isotherm and K is related to mean adsorption energy (E in kJ/mol) given by:

$$E = \frac{1}{\sqrt{2K}} \tag{14}$$

A plot of $\ln q_e$ versus ε^2 will give the value of maximum adsorption capacity of q_m (mg/g) from the intercept, and the value of K from the slope (plot not shown). If the E value lies between 1 and 8 kJ/mol, this indicates a physical adsorption whereas for chemical adsorption, the E value should be greater than 16 kJ/mol. If the E value is between 8 and 16 kJ/mol, ion-exchange will be the most likely adsorption mechanism involved (Erdem et al., 2004). Based on the mean adsorption energy (E) value of 20.4 kJ/mol (Table 2), the adsorption mechanism of lead ions onto CTRL could also involve chemical adsorption.

Table 3 shows the values of adsorption capacity (q_{max}) for the adsorption of lead ions on different adsorbents cited in the literature compared with that of the present study. Remarkably, CTRL has a much higher value of adsorption capacity compared to other adsorbents. This is an indication that CTRL is a promising adsorbent for treating wastewater containing lead ions since rubber leaves are relatively abundant and the method of modification is simple, yet very effective.

3 Conclusions

Rubber leaf powder treated with potassium permanganate followed by sodium carbonate showed good adsorption capacity of lead ions. Adsorption capacity was affected at low pH and higher adsorbent dosage but increased with increase in concentration and contact time. Lead adsorption obeyed the pseudo second-order kinetic model while equilibrium data presented a better fitting to the Langmuir isotherm model. The FT-IR analysis revealed –OH, –NH$_2$, –COOH, C=C and –COO$^-$ as the

Table 3　Comparison of adsorption capacity of CTRL for Pb(II) ions with other adsorbents

Adsorbent	Source of adsorbent	q_{max} (mg/g)	Reference
CTRL	Agricultural waste	95.3	This study
Bacillus sp.	Microorganism	92.3	Tunali et al., 2006
Wheat bran	Agricultural waste	87.0	Bulut and Baysal, 2006
Zeolite tuff	Mineral	68.0	Wang et al., 2008
Activated carbon (Palm shell)	Agricultural waste	53.5	Yin et al., 2008
Black gram husk	Agricultural waste	49.9	Saeed et al., 2005
Myriophyllum spicatum	Aquatic plant	46.5	Keskinkan et al., 2003
Spent grain	Agricultural waste	35.0	Li et al., 2009
Nopal (*Opuntia streptacantha*)	Agricultural waste	28.9	Miretzky et al., 2008
Chinese herb Pang Da Hai	Agricultural waste	27.1	Liu et al., 2006
Activated carbon (coconut shell)	Agricultural waste	26.5	Sekar et al., 2004
Coir	Agricultural waste	18.9	Conrad and Hansen, 2007
Bentonite	Clay	14.5	Donat et al., 2005
Rice husk ash	Agricultural waste	12.6	Feng et al., 2004
Sericite	Clay	4.7	Tiwari et al., 2007

major functional groups that act as adsorption sites for lead ions. Chemical adsorption and ion-exchange were the main adsorption mechanisms involved as indicated by D-R isotherm, FT-IR and EDX spectra.

References

Akar T, Tunali S, 2005. Biosorption performance of *Botrytis cinerea* fungal by-products for removal of Cd(II) and Cu(II) ions from aqueous solutions. *Minerals Engineering*, 18: 1099–1109.

Arief V O, Trilestari K, Sunarso J, Indraswati N, Ismadji S, 2008. Recent progress on biosorption of heavy metals from liquids using low cost biosorbents: Characterization, biosorption parameters and mechanism studies. *Clean*, 36: 937–962.

Bailey S E, Olin T J, Bricka R M, Adrian D D, 1999. A review of potentially low-cost sorbents for heavy metals. *Water Research*, 33: 2469–2479.

Balasubramaniam R, Perumal S V, Vijayaraghavan K, 2009. Equilibrium isotherm studies for the multicomponent adsorption of lead, zinc, and cadmium onto Indonesian peat. *Industrial and Engineering Chemistry Research*, 48: 2093–2099.

Balistrieri L S, Murray J W, 1981. The surface chemistry of goethite (α-FeOOH) in major ion seawater. *American Journal of Science*, 281: 788–806.

Basha S, Murthy Z V P, Jha B, 2008. Biosorption of hexavalent chromium by chemically modified seaweed, *Cystoseira indica*. *Chemical Engineering Journal*, 137: 480–488.

Basha S, Murthy Z V P, 2007. Kinetic and equilibrium models for biosorption of Cr(VI) on chemically modified seaweed, *Cystoseira indica*. *Process Biochemistry*, 42: 1521–1529.

Bulut Y, Baysal Z, 2006. Removal of Pb(II) from wastewater using wheat bran. *Journal of Environmental Management*, 78: 107–113.

Bulut Y, Tez Z, 2007. Adsorption studies on ground shells of hazelnut and almond. *Journal of Hazardous Materials*, 149: 35–41.

Boyd G E, Adamson A M, Myers Jr L S, 1947. The exchange adsorption of ions from aqueous solutions by organic zeolites,

II: kinetics. *Journal of the American Chemical Society*, 69: 2836–2848.

Conrad K, Hansen H C B, 2007. Sorption of zinc and lead on coir. *Bioresource Technology*, 98: 89–97.

Donat R, Akdogan A, Erdem E, Cetisli H, 2005. Thermodynamics of Pb^{2+} and Ni^{2+} adsorption onto natural bentonite from aqueous solutions. *Journal of Colloid and Interface Science*, 286: 43–52.

Dubinin M M, Zaverina E D, Radushkevich L V, 1947. Sorption and structure of active carbons. I. Adsorption of organic vapors. *Journal of Physical Chemistry*, 21: 1351–1362

Erdem E, Karapinar N, Donat R, 2004. The removal of heavy metal cations by natural zeolites. *Journal of Colloid and Interface Science*, 280: 309–314.

Farinella N V, Matos G D, Arruda M A Z, 2006. Grape bagasse as a potential biosorbent of metals in effluent treatments. *Bioresource Technology*, 98: 1940–1946.

Feng Q, Lin Q, Gong F, Sugita S, Shoya M, 2004. Adsorption of lead and mercury by rice husk ash. *Journal of Colloid and Interface Science*, 278: 1–8.

Freundlich H M F, 1906. Über die adsorption in läosungen. *Journal of Physical Chemistry*, 57: 385–470.

Giles C H, Smith D, Huitson A, 1974. A general treatment and classification of the solute adsorption isotherm. I. Theoretical. *Journal of Colloid and Interface Science*, 47: 755–765.

Gupta S S, Bhattacharyya K G, 2008. Immobilization of Pb(II), Cd(II) and Ni(II) ions on kaolinite and montmorillonite surfaces from aqueous medium. *Journal of Environmental Management*, 87: 46–58.

Hanafiah M A K M, Zakaria H, Wan Ngah W S, 2009. Preparation, characterization, and adsorption behavior of Cu(II) ions onto alkali-treated weed (*Imperata cylindrica*) leaf powder. *Water, Air, and Soil Pollution*, 201: 43–53.

Hanafiah M A K M, Ngah W S W, Ibrahim S C, Zakaria H, Ilias W A H W, 2006. Kinetics and thermodynamic study of lead adsorption from aqueous solution onto rubber (*Hevea brasiliensis*) leaf powder. *Journal of Applied Sciences*, 6: 2762–2767.

Ho Y S, McKay G, 1998. A comparison of chemisorption kinetic models applied to pollutant removal on various sorbents. *Process Safety and Environmental Protection*, 76: 332–340.

Ho Y S, McKay G, 2000. The kinetics of sorption of divalent metal ions onto sphagnum moss peat. *Water Research*, 34: 735–742.

Ho Y S, Porter J S, McKay G, 2002. Equilibrium isotherm studies for the sorption of divalent metal ions onto peat: Copper,

nickel and lead single component systems. *Water, Air, and Soil Pollution*, 141: 1–33.

Kadirvelu K, Namasivayam C, 2003. Activated carbon from coconut coir pith as metal adsorbent: Adsorption of Cd(II) from aqueous solution. *Advances in Environmental Research*, 7: 471–478.

Keskinkan O, Goksu M Z L, Yuceer A, Basibuyuk M, Forster C F, 2003. Heavy metal adsorption characteristics of a submerged aquatic plant. *Process Biochemistry*, 39: 179–183.

Langmuir I, 1916. The constitution and fundamental properties of solids and liquids. *Journal of the American Chemical Society*, 38: 2221–2295.

Lee S H, Shon J S, Chung H, Lee M Y, Yang J W, 1999. Effect of chemical modification of carboxyl groups in apple residues on metal ion binding. *Korean Journal of Chemical Engineering*, 16: 576–580.

Lesmana S O, Febriana N, Soetaredjo F E, Sunarso J, Ismadji S, 2008. Studies on potential applications of biomass for the separation of heavy metals from water and wastewater. *Biochemical Engineering Journal*, 44: 19–41.

Li Q Z, Chai L Y, Yang Z H, Wang Q W, 2009. Kinetics and thermodynamics of Pb(II) adsorption onto modified spent grain from aqueous solutions. *Applied Surface Science*, 255: 4298–4303.

Liu Y H, Cao Q L, Luo F, Chen Ji, 2009. Biosorption of Cd^{2+}, Cu^{2+}, Ni^{2+} and Zn^{2+} ions from aqueous solutions by pretreated biomass of brown algae. *Journal of Hazardous Materials*, 163: 931–938.

Liu Y, Chang X, Guo Y, Meng S, 2006. Biosorption and precon-centration of lead and cadmium on waste Chinese herb Pang Da Hai. *Journal of Hazardous Materials*, B135: 389–394.

Luo F, Liu Y, Li X, Xuan Z, Ma J, 2006. Biosorption of lead ion by chemically-modified biomass of marine brown algae Laminaria japonica. *Chemosphere*, 64: 1122–1127.

Malkoc E, Nuhoglu Y, 2005. Investigations of nickel(II) removal from aqueous solutions using tea factory waste. *Journal of Hazardous Materials*, 127: 120–128.

Miretzky P, Muñoz C, Carrilho-Chávez A, 2008. Experimental binding of lead to a low cost on biosorbent: Nopal (*Opuntia streptacantha*). *Bioresource Technology*, 99: 1211–1217.

Ncibi M C, Mahjoub B, Seffen M, 2006. Studies on the biosorp-tion of textile dyes from aqueous solutions using *Posidonia oceanica* (L.) leaf sheath fibres. *Adsorption Science and Technology*, 24: 461–473.

O'Connell D W, Birkinshaw C, O'Dwyer T F, 2008. Heavy metal adsorbents prepared from the modification of cellulose: A review. *Bioresource Technology*, 99: 6709–6724.

Ozsoy H D, Kumbur H, 2006. Adsorption of Cu(II) ions on cotton ball. *Journal of Hazardous Materials*, 136: 911–916.

Panda G C, Das S K, Bandopadhyay T S, Guha A K, 2007. Adsorption of nickel on husk of *Lathyrus sativus*: Behavior and binding mechanism. *Colloids and Surfaces B: Biointer-faces*, 57: 135–142.

Pino G H, de Mesquita L M S, Torem M L, Pinto G A S, 2006. Biosorption of cadmium by green coconut shell powder. *Minerals Engineering*, 19: 380–387.

Saeed A, Iqbal M, Akhtar M W, 2005. Removal and recovery of lead(II) from single and multimetal (Cd, Cu, Ni, Zn) solutions by crop milling waste (black gram husk). *Journal of Hazardous Materials*, B117: 65–73.

Sekar M, Sakthi V, Rengaraj S, 2004. Kinetics and equilibrium adsorption study of lead(II) onto activated carbon prepared from coconut shell. *Journal of Colloid and Interface Science*, 279: 307–313.

Shukla A, Zhang Y H, Dubey P, Margrave J L, Shukla S S, 2002. The role of sawdust in the removal of unwanted materials from water. *Journal of Hazardous Materials*, B95: 137–152.

Tiwari D, Kim H U, Lee S M, 2007. Removal behavior of sericite for Cu(II) and Pb(II) from aqueous solutions: Batch and column studies. *Separation and Purification Technology*, 57: 11–16.

Tunali S, Çabuk A, Akar T, 2006. Removal of lead and copper ions from aqueous solutions by bacterial strain isolated from soil. *Chemical Engineering Journal*, 115: 203–211.

Upendra K, Bandyopadhyay M, 2006. Sorption of cadmium from aqueous solution using pretreated rice husk. *Bioresource Technology*, 97: 104–109.

Vijayaraghavan K, Palanivelu K, Velan M, 2006. Biosorption of copper(II) and cobalt(II) from aqueous solutions by crab shell particles. *Bioresource Technology*, 97: 1411–1419.

Wan Ngah W S, Hanafiah M A K M, 2009. Surface modification of rubber (*Hevea brasiliensis*) leaves for the adsorption of copper ions: kinetic, thermodynamic and binding mecha-nisms. *Journal of Chemical Technology and Biotechnology*, 84: 192–201.

Wan Ngah W S, Hanafiah M A K M, 2008a. Removal of heavy metal ions from wastewater by chemically modified plant wastes as adsorbents: A review. *Bioresource Technology*, 99: 3935–3948.

Wan Ngah W S, Hanafiah M A K M, 2008b. Adsorption of copper on rubber (*Hevea brasiliensis*) leaf powder: Kinetic, equilibrium and thermodynamic studies. *Biochemical Engi-neering Journal*, 39: 521–530.

Wan Ngah W S, Hanafiah M A K M, 2008c. Biosorption of copper ions from dilute aqueous solutions on base treated rubber (*Hevea brasiliensis*) leaves powder: kinetics, isotherm, and biosorption mechanisms. *Journal of Environ-mental Sciences*, 20(10): 1168–1176.

Wang S, Terdkiatburana T, Tad M O, 2008. Adsorption of Cu(II), Pb(II) and humic acid on natural zeolite tuff in single and binary systems. *Separation and Purification Technology*, 62: 64–70.

Yin C Y, Aroua M K, Wan Daud W M A, 2008. Enhanced ad-sorption of metal ions onto polyethyleneimine-impregnated palm shell activated carbon: Equilibrium studies. *Water, Air, and Soil Pollution*, 192: 337–348.